Spectral analysis of gravity wave activity in SABER temperature data

Marc Krebsbach[1,2] and Peter Preusse[1]

Received 1 September 2006; revised 7 November 2006; accepted 9 January 2007; published 10 February 2007.

[1] Since January 2002, the SABER (Sounding of the Atmosphere using Broadband Emission Radiometry) instrument has performed continuous measurements from near the tropopause into the thermosphere. For the time period 29 January 2002–31 January 2006, we spectrally analyzed time series of weekly zonal root mean square gravity wave (GW) amplitudes for systematic intra-annual, annual and inter-annual GW activity. GWs considered have horizontal wavelengths between 100 km and zonal wave number 6 and vertical wavelengths between 5–30 km. Height-latitude cross sections of spectral amplitudes and phases between 20–100 km and 55°S–55°N show several relevant oscillations. A strong semiannual variation is evident in the high-latitude upper stratosphere/mesosphere. Annual components reveal two isolated maxima at mid-latitudes in both hemispheres, associated with the winter polar vortices, and summertime maxima in the subtropics. Biennial amplitudes in the equatorial stratosphere coincide with the descending westerly shear phase and can be attributed to the quasi-biennial oscillation. **Citation:** Krebsbach, M., and P. Preusse (2007), Spectral analysis of gravity wave activity in SABER temperature data, *Geophys. Res. Lett.*, *34*, L03814, doi:10.1029/2006GL028040.

1. Introduction

[2] Middle atmosphere winds are accelerated by the momentum transfer of dissipating gravity waves (GWs) and in particular intra-annual and inter-annual oscillations are partly maintained by GWs. For instance, mesoscale and large scale GWs should contribute the same or a larger amount to the driving of the quasi-biennial oscillation (QBO) as the large scale Kelvin and Rossby gravity waves [*Dunkerton*, 1997]. Also the mesospheric semiannual oscillation (SAO) and the intra-annual variation of tidal amplitudes is at least partly attributed to GWs [*Mayr et al.*, 1998a, 1998b]. On the other hand these wind systems filter the GW spectrum and according variations of GW activity are expected. Variations might then affect altitude and latitude ranges different from those where e.g. the QBO is generated.

[3] A QBO signal in GW activity has been identified in GPS-RO observations at equatorial latitudes in the lower stratosphere [*Wu*, 2006; *de la Torre et al.*, 2006]. However, GPS data are limited to the lower and middle stratosphere. A four year continuous data set of temperatures retrieved from the SABER (Sounding of the Atmosphere using Broadband Emission Radiometry) instrument on TIMED (Thermosphere Ionosphere Mesosphere Energetics Dynamics) now provides the opportunity to make a systematic survey of long-term variations in GW activity through the whole middle atmosphere.

[4] In this paper we use a selected time period from the long-term SABER temperature data record (29 January 2002–31 January 2006, i.e. 209 weeks) to perform a spectral analysis of GWs. The multi-year time series allows for identification of systematic intra-annual, annual and inter-annual structures of GW activity.

2. Spectral Analysis of Gravity Wave Activity

[5] Version 1.06 temperature data from SABER (level 2A) are available since the beginning of 2002 and provide a more than 4 years continuous coverage (without gaps) for latitudes between 52°S and 52°N, thus allowing spectral analysis of intra-annual, annual and inter-annual GW activity.

2.1. Isolation of Gravity Waves

[6] To isolate GWs from other dynamical atmospheric signatures we use a technique introduced by *Fetzer and Gille* [1994] and subtract a background atmosphere estimated by a zonal wave number 0–6 Kalman filter. A detailed discussion of the advantages and limitations of this technique has recently been given in Appendix A of *Ern et al.* [2006]. Resulting residual temperatures contain signals from GWs with horizontal wavelengths longer than the visibility limit of 100 km [*Preusse et al.*, 2002] up to several 1000 km. Tidal signatures are removed by detrending ascending and descending orbit legs separately as discussed by *Preusse et al.* [2001]. Residual temperatures are calculated on a vertical grid of 800 m oversampling the 2 km wide field of view of SABER. Vertical profiles are analyzed by a combination of Maximum Entropy Method and sinusoidal fits (SF) described by *Preusse et al.* [2002], resulting in amplitude, phase and vertical wavelength of the two leading wave components at every altitude of the height profiles. The SF window is chosen to be 10 km and limits the vertical resolution of the amplitude structures described in this paper [cf. *Preusse et al.*, 2002, section 3]. Furthermore, the limitations due to the vertical resolution allowing analyses of waves with $\lambda_z > 5$ km has to be taken into account when data are interpreted e.g. in model comparisons [*Alexander*, 1998; *Ern et al.*, 2006].

2.2. Spectral Analysis

[7] For the systematic survey, the data is binned in cells of 10° in latitude, overlapping each other by 5°. The altitude range between 20 km and 100 km is subdivided in 2 km steps. Weekly zonal means of GW squared amplitudes are calculated, whereby different ranges of λ_z are considered. The square root values of these weekly zonal means (i.e.,

[1]Institut I: Stratosphäre, Institut für Chemie und Dynamik der Geosphäre, Forschungszentrum Jülich GmbH, Jülich, Germany.
[2]Now at Faculty of Mathematics and Natural Sciences, Physics Department, University of Wuppertal, Wuppertal, Germany.

Copyright 2007 by the American Geophysical Union.
0094-8276/07/2006GL028040

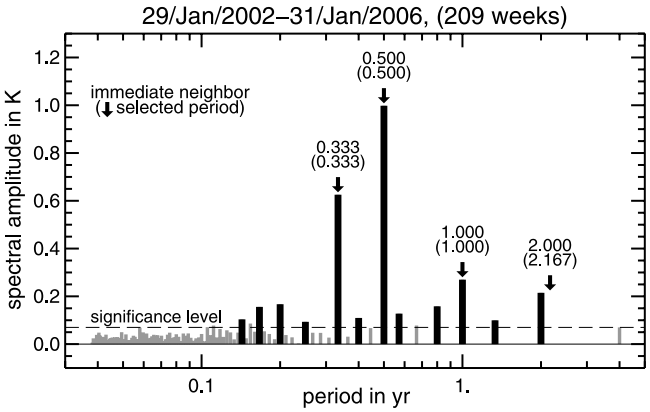

Figure 1. Example spectrum of performed FFT for vertical wavelengths between 5 km and 30 km in the latitude band 30.0S ± 2.5° and altitude range 60.0 ± 1.0 km. Spectral amplitudes above the significance level of 1.3 times the average spectral amplitude ($1.3 \times \hat{A}$, dashed line) are marked by vertical black boldface bars.

weekly zonal root mean square GW amplitudes, WZRMS) are merged to a time series. By using WZRMS, we avoid (i) an overemphasis of single high values and (ii) a logarithmic color scale in the result plots. The WZRMS time series is spectrally analyzed by applying a Fast Fourier Transformation (FFT). Below, we concentrate on the results for λ_z between 5 and 30 km and discuss differences to distributions of GW ensembles of shorter and longer λ_z.

[8] As an example, Figure 1 shows the outcome of the performed FFT for λ_z between 5 km and 30 km for 30.0S ± 2.5° latitude and 60.0 ± 1.0 km altitude.

[9] In order to identify relevant spectral components, we define a significance criterion of 1.3 times the average of all spectral components, and consider all spectral amplitudes exceeding $1.3 \times \hat{A}$ (dashed line) to be significant. Since the time period covers 4 years, the selected intra-annual and annual periods fall onto the periods covered by the FFT. Instead of the mean QBO period of 26 months we discuss the immediate neighbor period of 2 years. The example shows that the selected terannual, semiannual, annual and biennial periods clearly emerge from the background and the adjacent periods.

2.3. Description of Examined Spectral Components

[10] In the following, we present spectral amplitudes and phases of GW square-mean amplitudes for selected periods as a function of altitude and latitude. As illustrated in Figure 1, the terannual period is significant in a wide range of altitudes and latitudes. Furthermore, the quarterly periodicity is often significant. For a comprehensive overview, however, we focus on periods of 0.5, 1.0, and 2.0 years. The cross sections cover the altitude region between 20 km and 100 km within the latitude band 55°S–55°N. Figure 2 shows altitude latitude cross sections of spectral amplitudes (left column, in K) and phases of the wave maximum given in months with respect to 1 January 2002 (right column). Please note that for altitudes above ≈80 km it can not be ensured whether temperature variations can solely be assigned to GWs or have to be attributed to other thermodynamic processes relevant in this height region. These altitudes are shown for completeness but not further discussed.

2.3.1. Semiannual Period

[11] It is not possible to state whether the observed semiannual variations are causing an annual or semiannual oscillation in the exerted GW drag. If for instance, waves propagate preferentially eastward in summer and westward in winter with quiet equinoxes, this will cause an annual variation in wave acceleration, but we will observe two maxima and hence a semiannual variation in wave amplitudes. In order to resolve this question, information on the wave propagation direction would be required.

[12] Semiannual variations exceed the level of significance in all considered regions except in the tropical lower and middle stratosphere. The amplitude distribution is nearly symmetric about the equator. Low latitude semiannual variations increase with height from 0.3 K at 40 km to 0.6 K at 70 km with downward propagating phase and decrease above. Large amplitudes >2 K are evident in the considered height region above 90 km between 55°S and 40°N which are primarily attributed to variations with $\lambda_z > 15$ km.

[13] The observed semiannual variations are much stronger at mid-latitudes. This is consistent with previous SAO observations of mean temperatures. The wintertime wind field in the mesosphere and lower thermosphere is marked by a strong variability, essentially in consequence of processes occurring in the stratosphere (e.g., stratospheric warmings, enhanced activity of planetary waves). A superposition of wintertime pulses and summertime heating will lead to strong semiannual components [e.g., *Gao et al.*, 1987]. The stratospheric high latitude semiannual variation is stronger in the SH than in the NH. In the SH mesosphere, spectral amplitudes up to 1.8 K are evident. A similar mesospheric structure is apparent in the NH albeit with distinctly reduced amplitude. These two maxima are connected in the mesosphere with a crescent-shaped region of enhanced amplitudes, decreasing in magnitude towards the equator. This structure is even more revealed in Figure 2c, presenting spectral amplitudes of GWs with λ_z between 5 and 15 km. Half of size of the semiannual amplitudes can be attributed to GWs with $\lambda_z \leq 15$ km. Higher amplitudes appear near the solstices. No enhanced amplitudes are found during the equinoxes.

2.3.2. Annual Period

[14] The dominant patterns of annual variability are two relatively isolated amplitude maxima in mid-latitudes of both hemispheres. The defined enhancements at latitudes greater than 40° are obviously correlated to high wind speeds [*Alexander*, 1998] of the westerly mesospheric (65 km) and stratospheric (30 km) jet streams near 60° associated with the winter polar vortices. As discussed in detail by *Preusse et al.* [2006], reasons for such correlations are likely favorable propagation conditions and high saturation amplitudes for upward propagating waves amplified by shifting slow phase speed waves into the visibility range of the instrument. These GW active regions with spectral amplitudes >2 K in the northern and southern hemisphere reach from 30 km up to about 80 km with the maxima around 60 and 65 km, respectively. Annual enhancements are more intense in the SH (>3.5 K), possibly due to the

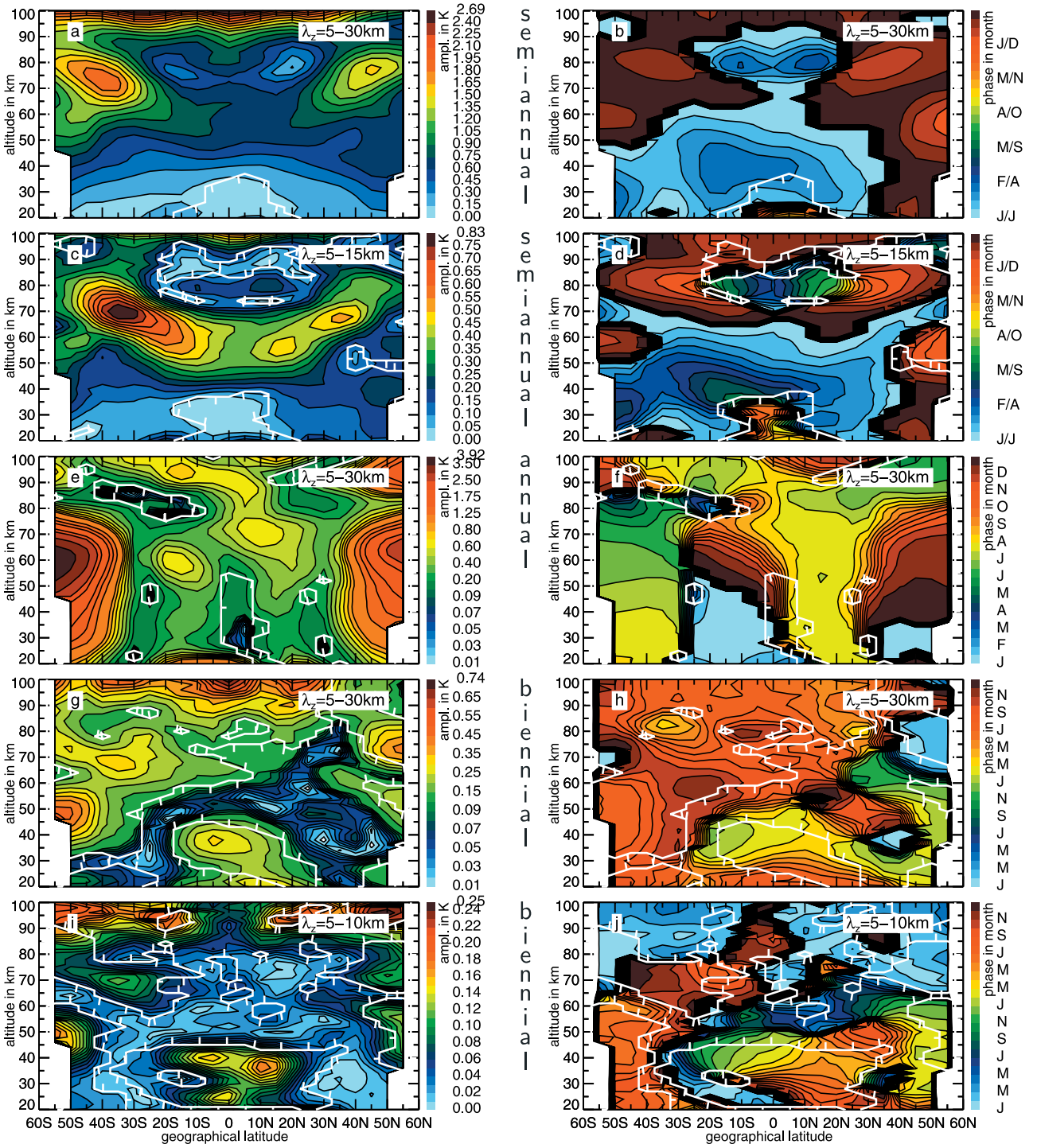

Figure 2. Altitude-latitude sections of (left) spectral amplitudes (color coded in K) and (right) phases for different periods (color coded in months, shifted to January 1, 2002). Spectral amplitudes of weekly zonal square-mean GW amplitudes are shown for vertical wavelength ranges (a, b, e–h) 5–30 km, (c, d) 5–15 km, and (i, j) 5–10 km. Three periods are selected (top to bottom): 0.5 (semiannual variation), 1.0 (annual variation), 2.0 years (biennial variation). Areas regarded as significant ($1.3 \times \hat{A}$) are uphill of the white contour.

larger size and strength of the southern polar vortex. Associated phases reveal a coincidence with a descending polar vortex during October to January in the NH and during May to August in the SH. The downward propagating phases have little latitudinal variation within 55–30°S and 30–55°N, whereby the constant phase structure is more definite in the SH compared to the NH. This suggests long lasting events of high amplitudes at these latitudes and that the latitudinal variation of GW activity depends on both, hemisphere and season.

[15] At lower latitudes, increased amplitudes of 0.6 K are apparent near 15°S in 60 km with downward propagating

phase (November–December) and at 10°N in 70 km altitude with quasi constant phase (July), respectively. In the respective subtropical summer hemisphere, there are two possible reasons for enhanced GWs. First, a high correlation between wind speeds and GW activity is well reputed [e.g., *Alexander*, 1998; *Preusse et al.*, 2006]. Second, convection acts as a source of GW excitations [*Jiang et al.*, 2004; *Preusse and Ern*, 2005].

[16] Below 30 km altitude, elevated annual spectral amplitudes are not symmetric about the equator. Enhancements are found in the subtropic convection regions in summertime NH (end of July, 15–30°N), which possibly correspond to the continental regions of Africa, Asia and Mexico [cf. *Alexander*, 1998]. During the equatorial wet season, the broader subtropic/tropic convection regions of the summertime SH (January–February, 25°S–5°N) are apparent in the amplitude distributions, supposedly also attributed to convection. A considerable decrease of annual spectral amplitudes occurs in the equatorial region between 25–50 km height, which is labeled as an insignificant area.

2.3.3. Biennial Period

[17] Compared to annual variations spectral amplitudes for a period of 2 years are weak. Generally, biennial variations are more extended in the SH than in the NH, at least in the zonal means. Significant magnitudes of at most 0.3 K occur in the equatorial stratosphere. Phases are propagating downwards from January to July of the second years. These years, 2003 and 2005, coincide with the easterly phase of the QBO when winds are considerably stronger than during the westerly phase (updated by *Naujokat* [2005] from *Naujokat* [1986]). The related phases of enhanced amplitudes correspond to the descending westerly shear phase of QBO winds [e.g., *Randel and Wu*, 2005]. These largest contributions of spectral amplitudes, which are not apparent in the annual and semiannual variations, suggest an influence of the equatorial QBO on GW activity.

[18] Resulting distributions of spectral amplitudes and phases for GWs with λ_z between 5 and 10 km are illustrated in Figures 2i and 2j. Enhanced amplitudes in the equator stratosphere show a downward propagating phase of $\approx$11 months from April to March, which is in close agreement to GPS-RO observations of the same GW wavelengths [*de la Torre et al.*, 2006].

[19] Further enlarged amplitudes are apparent in both hemispheres near 50° at 50 km and 70 km altitude. Associated phases correspond to the respective winter seasons. An interference of the biennial variation with the polar vortices is likely [e.g., *Baldwin et al.*, 2001]. The distribution shows a stronger influence in the southern stratospheric polar vortex and in the NH mesosphere.

2.4. Comparison to Other Methods

[20] Comparisons to other techniques can help to solve the ambiguity of a GW variance SAO signal. *Gavrilov et al.* [2003] reported about radar measurements above Hawaii (20°N). Longer period GWs (their Figure 10) show an annual oscillation at 76 km with maximum in summer vanishing above (consistent with a drop in amplitude in our Figure 2e) and a semiannual component with increasing amplitude above 80 km with maxima shifting from January/July at 80 km to March/August at 92 km (consistent with our Figures 2a and 2b).

[21] Air glow imager measurements [*Tang et al.*, 2005] observe short horizontal wavelength GWs unlikely to be measured by SABER, but give information on the propagation direction. Qualitative information like the propagation direction could be comparable for the two instruments, if the dominant process is wind filtering, since wind filtering depends mostly on the horizontal phase speed and only very weakly on the horizontal wavelength. For two stations at Hawaii and New Mexico they indicate a direction reversal from northeastward in summer to southwestward in winter, indicating that for the subtropics the observed SAO in wave variance is actually an annual variation in GW momentum. The different phase behavior at latitudes 20°S–20°N indicates that in the tropics we observe a true SAO signal and that Hawaii is just at the transition of the two regimes.

3. Concluding Remarks

[22] The SABER instrument provides an ongoing multiyear record of the structure of the middle atmosphere with a high potential to analyze temporal periodicities of GW amplitudes. Height-latitude cross sections of spectral amplitudes and phases show salient features in intra-annual, annual and inter-annual GW variability. Mesospheric QBO and SAO are believed to be forced by GWs filtered in the stratosphere. Accordingly, we observe QBO and SAO signals in the mesospheric analyses, which are however smaller than the variations at higher latitudes. This might be partly due to the fact that we observe GW variances, not momentum flux, and possibly due to the limited altitude resolution.

[23] A full understanding of the presented data will require modeling studies taking into account the wavelength limits implied by the measurement and analysis technique. To affirm the observed morphologies, the analysis might be improved by using a longer time series in the future.

[24] **Acknowledgments.** We thank the whole SABER team, in particular R. H. Picard, M. G. Mlynczak, J. M. Russel III and L. L. Gordley for useful discussions of SABER data. This work is funded by the Deutsche Forschungsgemeinschaft (DFG), project GW-CODE (ER 474/1-1), DFG priority program CAWSES SPP 1176.

References

Alexander, M. J. (1998), Interpretations of observed climatological patterns in stratospheric gravity wave variance, *J. Geophys. Res.*, *103*, 8627–8640.

Baldwin, M. P., et al. (2001), The quasi-biennial oscillation, *Rev. Geophys.*, *39*(2), 179–229.

de la Torre, A., T. Schmidt, and J. Wickert (2006), A global analysis of wave potential energy in the lower stratosphere derived from 5 years of GPS radio occultation data with CHAM, *Geophys. Res. Lett.*, *33*, L24809, doi:10.1029/2006GL027696.

Dunkerton, T. J. (1997), The role of gravity waves in the quasi-biennial oscillation, *J. Geophys. Res.*, *102*, 26,053–26,076.

Ern, M., P. Preusse, and C. D. Warner (2006), Some experimental constraints for spectral parameters used in the Warner and McIntyre parameterization scheme, *Atmos. Chem. Phys.*, *6*, 4361–4381.

Fetzer, E. J., and J. C. Gille (1994), Gravity wave variances in LIMS temperatures: I. Variability and comparison with background winds, *J. Atmos. Sci.*, *51*, 2461–2483.

Gao, X.-H., W.-B. Yu, and L. Stanford (1987), Global features of the semiannual oscillation in stratospheric temperatures and comparison between seasons and hemispheres, *J. Atmos. Sci.*, *44*, 1041–1048.

Gavrilov, N. M., D. M. Riggin, and D. C. Fritts (2003), Medium-frequency radar studies of gravity-wave seasonal variations over Hawaii (22°N, 160°W), *J. Geophys. Res.*, *108*(D20), 4655, doi:10.1029/2002JD003131.

Jiang, J. H., B. Wang, K. Goya, K. Hocke, S. D. Eckermann, J. Ma, D. L. Wu, and W. G. Read (2004), Geographical distribution and interseasonal

variability of tropical deep convection: UARS MLS observations and analyses, *J. Geophys. Res.*, *109*, D03111, doi:10.1029/2003JD003756.

Mayr, H. G., J. G. Mengel, and K. L. Chan (1998a), Equatorial oscillations maintained by gravity waves as described with the Doppler spread parameterization: I. Numerical experiments, *J. Atmos. Sol. Terr. Phys.*, *60*, 181–199.

Mayr, H. G., J. G. Mengel, K. L. Chan, and H. S. Porter (1998b), Seasonal variations of the diurnal tide induced by gravity wave filtering, *Geophys. Res. Lett.*, *25*, 943–946.

Naujokat, B. (1986), An update of the observed quasi-biennial oscillation of the stratospheric winds over the tropics, *J. Atmos. Sci.*, *43*, 1873–1877.

Naujokat, B. (2005), Variability of the stratosphere: The QBO, *Promet*, *31*(1), 30–32.

Preusse, P., and M. Ern (2005), Indication of convectively generated gravity waves observed by CLAES, *Adv. Space Res.*, *35*, 1987–1991, doi:10.1016/j.asr.2004.09.005.

Preusse, P., S. D. Eckermann, J. Oberheide, M. E. Hagan, and D. Offermann (2001), Modulation of gravity waves by tides as seen in CRISTA temperatures, *Adv. Space Res.*, *27*, 1773–1778.

Preusse, P., A. Dörnbrack, S. D. Eckermann, M. Riese, B. Schaeler, J. T. Bacmeister, D. Broutman, and K. U. Grossmann (2002), Space-based measurements of stratospheric mountain waves by CRISTA 1: Sensitivity, analysis method, and a case study, *J. Geophys. Res.*, *107*(D23), 8178, doi:10.1029/2001JD000699.

Preusse, P., et al. (2006), Tropopause to mesopause gravity waves in August: Measurement and modeling, *J. Atmos. Sol. Terr. Phys.*, *68*, 1730–1751.

Randel, W. J., and F. Wu (2005), Kelvin wave variability near the equatorial tropopause observed in GPS radio occultation measurements, *J. Geophys. Res.*, *110*, D03102, doi:10.1029/2004JD005006.

Tang, J., G. R. Swenson, A. Z. Liu, and F. Kamalabadi (2005), Observational investigations of gravity wave momentum flux with spectroscopic imaging, *J. Geophys. Res.*, *110*, D09S09, doi:10.1029/2004JD004778.

Wu, D. L. (2006), Small-scale fluctuations and scintillations in high-resolution GPS/CHAMP SNR and phase data, *J. Atmos. Sol. Terr. Phys.*, *68, 999–1017.*

M. Krebsbach, Faculty of Mathematics and Natural Sciences, Physics Department, University of Wuppertal, D-42119 Wuppertal, Germany. (m.krebsbach@uni-wuppertal.de)

P. Preusse, Institut I: Stratosphäre, Institut für Chemie und Dynamik der Geosphäre, Forschungszentrum Jülich GmbH, D-52425 Jülich, Germany.